Electromagnetic Radial Diffusion in the Earth's Radiation Belts as Determined by the Solar Wind Immediate Time History and a Toy Model for the Electromagnetic Fields

Solène Lejosne[1]

1. Space Science Laboratory, University of California, Berkeley

Corresponding author: S. Lejosne, solene@berkeley.edu

Keywords

Radial Diffusion – Radiation Belts – Solar Wind – Magnetopause – Turbulence

Key points

1. A model in which electromagnetic radial diffusion is determined by the immediate time history of the magnetopause location is presented.
2. With the magnetopause controlled by the solar wind, the diffusion coefficients per Kp index average similarly to the existing standard.
3. A time series of electromagnetic radial diffusion coefficients with a one-minute time resolution is provided for the year 2013.

Abstract

Diffusion-driven radiation belt models require multiple physics-based inputs to specify the radiation environment through which spacecraft travel, including diffusion coefficients. Even though event-specific coefficients are necessary for model accuracy, their routine integration in operational models has not yet been achieved. In fact, one of the key inputs, the radial diffusion coefficient, is still commonly determined by a Kp-driven parameterization.

This work presents a method to determine continuous time series of time-varying radial diffusion coefficients. A theoretical model is developed in which electromagnetic radial diffusion is controlled by the magnetopause immediate time history. Specifically, radial diffusion is described as a function of the average, variance, and autocorrelation time of the geocentric stand-off distance to the subsolar point on the magnetopause. Because the magnitudes of these three magnetopause parameters vary with time and magnetic activity, so does radial diffusion. To a lesser extent, radial diffusion is also controlled by the drift frequency of the radiation belt population. Moreover, radial diffusion is quantified using a standard model in which the magnetopause is controlled by the solar wind. Although the resulting diffusion coefficients span several orders of magnitude per Kp index, the median magnitudes are remarkably similar to the ones provided by the standard Kp-driven statistical parameterization.

Plain Language Summary

An increasing number of spacecraft operate through or within the terrestrial radiation belts, a region where charged energetic particles are trapped in the Earth's magnetic field. Computer codes simulate this dynamic radiative environment, with the objective of improving spacecraft design and understanding spacecraft anomalies. These codes are physics-based models. That is, they solve a master diffusion equation using a series of inputs that summarize the effects of different physical processes on particles. One of the key inputs to these codes is the radial diffusion coefficient. Yet its formulation is currently limited: It is an average, obtained by interpolating a few experimental data points, and the time resolution is no better than three hours. By detailing the physics underlying radial diffusion in a simple scenario, this work provides a new quantification for the radial diffusion coefficient. The time resolution is improved, and the coefficient variability is enhanced. The fact that the resulting coefficient varies around the standard values provided by the current reference adds credibility to the method. As a result, it is expected that this new quantification will contribute to improving the accuracy of radiation belt simulations.

1. Introduction

Diffusion-driven radiation belt models have been developed and operated since the mid-1990s (Beutier & Boscher, 1995) to specify the structure, intensity and variability of the radiation environment through which satellites operate (e.g., Horne et al., 2013). They consist of solving a diffusion equation to describe radiation belt dynamics (e.g, Schulz & Lanzerotti, 1974), based on the adiabatic theory of magnetically trapped particles (e.g. Northrop, 1963). Operating a physics-based radiation belt model requires quantifying different inputs, including radial diffusion.

Radial diffusion is a statistical characterization of the violation of the third adiabatic invariant for a trapped radiation belt population. It plays a key role in determining radiation belt dynamics, not only at Earth but also at the giant planets (e.g., Lejosne & Kollmann, 2019).

The most commonly used radial diffusion inputs for terrestrial radiation belt models are the empirical coefficients for electromagnetic radial diffusion determined by Brautigam and Albert (2000), and parameterized by the Kp index:

$$log_{10}\left(D_{LL}^{B\&A}/L^{10}\right) = -9.325 + 0.506 \times Kp \;\; [log_{10}(day^{-1})] \qquad (1)$$

where D_{LL} is the electromagnetic radial diffusion coefficient of a population of equatorial radiation belt particles, and the superscript "$B\&A$" stands for Brautigam and Albert's empirical law for radial diffusion. For non-equatorial particles of the same kinetic energy, the electromagnetic radial diffusion coefficient is proportional to the one in the equatorial case (Fälthammar, 1968; Schulz & Lanzerotti, 1974, p.89). Similar parameterization for equatorial electromagnetic radial diffusion was proposed by Ozeke et al. (2014) (Drozdov et al., 2017), based on the erroneous analytic expressions for radial diffusion developed by Fei et al. (2006) (Lejosne, 2019).

Brautigam and Albert's empirical law for electromagnetic radial diffusion presents advantageous features for operational models (e.g., Glauert et al., 2018). First, radiation belt simulations yield plausible results when using such formulation for radial diffusion (e.g., Kim et al., 2011). Second, the implementation of the formula is straightforward. Moreover, it provides uninterrupted (i.e., operational) evaluation of radial diffusion. On the other hand, even though the importance of using event-specific inputs to improve model accuracy is now recognized (e.g., Tu et al., 2009), their determination is seemingly incompatible with operational models. Indeed, the development of event-specific coefficients has called for intensive work so far: It requires running potentially costly numerical simulations (e.g., Li Z. et al., 2017), and/or carrying detailed analysis of specific data sets when available (e.g., Ali et al., 2016). Even so, uncertainty in the magnitude of these tailored, "event-specific" radial diffusion coefficients leads to uncertainty in the relative contribution of other processes to the observed particle distribution (e.g., Mann et al., 2016; Shprits et al., 2018; Mann et al., 2018). Such features hamper our ability to include event-specific radial diffusion coefficients in operational radiation belt models.

The objective of this work is to provide a method to build operational, event-specific, electromagnetic diffusion coefficients. It builds on the theoretical framework underlying Brautigam and Albert (2000)'s empirical formula for electromagnetic radial diffusion. The theoretical model is detailed in **Section 2**, together with its reformulation in terms of fluctuations of the magnetopause location. Applying Shue et al. (1998)'s magnetopause model, the magnitude and variability of the resulting radial diffusion coefficients are discussed in **Section 3**. **Section 4** presents the results in the case of the year 2013, together with a comparison with the electromagnetic radial diffusion coefficients estimated according to Brautigam and Albert (2000)'s formula. The approach is discussed **Section 5.**

2. Theoretical Model Description

2.1. Theoretical Framework Associated with Brautigam and Albert (2000)'s Formula for Electromagnetic Radial Diffusion

Brautigam and Albert (2000)'s empirical formula for electromagnetic radial diffusion is a least squares interpolation of experimental values obtained at $L = 4$ by Lanzerotti and Morgan (1973) and at $L = 6.6$ by Lanzerotti et al. (1978). In both cases, a time interval of one week to one month of magnetic field fluctuations was analyzed to quantify an analytic expression for electromagnetic radial diffusion. The analytic expression, developed by Fälthammar (1965; 1968), and further detailed by Schulz and Eviatar (1969), is the following:

$$\frac{D_{LL}}{L^{10}} = \frac{\Omega^2}{8}\left(\frac{5}{7}\right)^2 \frac{R_E^2}{B_E^2} P_A(\Omega) \qquad (2)$$

for equatorially mirroring particles, where $B_E \cong 0.3\ G$ is the magnetic equatorial field at the Earth surface, $R_E \cong 6400\ km$ is one Earth radius, $\Omega/2\pi$ is the trapped population drift frequency, and P_A is the power spectrum of the asymmetric field fluctuations of a simplified electromagnetic field model.

The magnetic field model is a magnetic dipole field to which a small perturbation is superimposed (Mead, 1964). The small perturbation is the sum of two components: a symmetric component, $S(t)$, independent of local time, φ, and an asymmetric component, $A(t)rcos\varphi$. An additional assumption connects both symmetric and asymmetric components of the magnetic field perturbation to the magnetopause location:

$$S(t) = \frac{B_1}{\mathscr{b}^3(t)} \tag{3}$$

and

$$A(t) = \frac{-B_2}{R_E \mathscr{b}^4(t)} \tag{4}$$

where $B_1 \cong 0.25\ G$ and $B_2 \cong 0.21\ G$, and $\mathscr{b} \sim 10\ R_E$ is the geocentric stand-off distance to the subsolar point on the magnetopause, normalized in units of Earth Radii (e.g., Schulz & Eviatar, 1969). As a result, the power spectrum of the asymmetric field fluctuations is proportional to the power spectrum of the symmetric field fluctuations, and the **equation (2)** for electromagnetic radial diffusion is also:

$$\frac{D_{LL}}{L^{10}} = 2\Omega^2 \left(\frac{5B_2}{21B_1B_E}\right)^2 \frac{1}{\mathscr{b}^2} P_S(\Omega) \tag{5}$$

Because a fluctuation of the magnetopause location, $\mathscr{b}'$, leads to a symmetric fluctuation of the magnetic field, S', that is about 10 times greater than the asymmetric one, A', ($A'R_E = -4B_2S'/(3B_1\mathscr{b}) \sim -0.1S'$), $P_S(\Omega)$ is more readily measurable than $P_A(\Omega)$. That is why the **equation (5)** is usually preferred to the **equation (2)** when it comes to evaluating radial diffusion experimentally (Lanzerotti & Morgan, 1973; Lanzerotti et al., 1978).

Alternatively, one can also reformulate **equation (2)** in terms of fluctuations in the magnetopause location since the magnitude of the magnetic field asymmetry is directly related to the magnetopause location (**equation (4)**).

2.2. Theoretical Model for Electromagnetic Radial Diffusion as Determined by the Magnetopause Location

Combining **equations (2) and (4)** yields:

$$\frac{D_{LL}}{L^{10}} = \frac{\Omega^2}{2}\left(\frac{20}{7}\right)^2 \left(\frac{B_2}{B_E}\right)^2 \frac{1}{\bar{\mathscr{b}}^{10}} \int_0^\infty \overline{\mathscr{b}'(0)\mathscr{b}'(u)} \cos(\Omega u)\, du \tag{6}$$

where $\bar{\mathscr{b}}$ is the average magnetopause location, $\mathscr{b}' = \mathscr{b} - \bar{\mathscr{b}}$ is the fluctuating part of the magnetopause location, and $\left(u \mapsto \overline{\mathscr{b}'(0)\mathscr{b}'(u)}\right)$ is the autocorrelation function of the

magnetopause location. Further assuming that the autocorrelation function of the magnetopause location is subject to an exponential decay:

$$\overline{\mathscr{b}'(0)\mathscr{b}'(u)} = \overline{\mathscr{b}'^2} e^{-u/\tau} \tag{7}$$

where τ is the fluctuation lifetime, and $\overline{\mathscr{b}'^2}$ is the variance of the signal. It results that:

$$\frac{D_{LL}}{L^{10}} = \frac{1}{2}\left(\frac{20}{7}\right)^2 \left(\frac{B_2}{B_E}\right)^2 \frac{\overline{\mathscr{b}'^2}}{\bar{\mathscr{b}}^{10}} \frac{\Omega^2\tau}{1+\Omega^2\tau^2} \tag{8}$$

Because radial diffusion coefficients are usually expressed on a logarithmic scale, let us focus on $log_{10}(D_{LL}/L^{10})$ in the remainder of the article:

$$log_{10}(D_{LL}/L^{10}) = -10log_{10}(\bar{\mathscr{b}}) + log_{10}\left(\overline{\mathscr{b}'^2}\right) + log_{10}\left(\frac{\Omega^2\tau}{1+\Omega^2\tau^2}\right) + C \tag{9}$$

where

$$C = log_{10}\left(\frac{1}{2}\left(\frac{20}{7}\right)^2 \left(\frac{B_2}{B_E}\right)^2\right) \cong 0.3 \tag{10}$$

is a constant. The third term on the right-hand side of **equation (9)** is the only term that explicitly depends on the kinetic energy of the trapped population. It reaches a maximum equal to $-log_{10}\tau$ at very high energies, when $\Omega\tau \gg 1$. On the other hand, assuming that the fluctuation lifetime is very small in comparison with the radiation belt population drift period ($\Omega\tau \ll 1$), **equation (9)** becomes:

$$log_{10}(D_{LL}/L^{10}) = F\left(\bar{\mathscr{b}}; \overline{\mathscr{b}'^2}; \tau\right) + 2log_{10}\Omega + C \tag{11}$$

where

$$F\left(\bar{\mathscr{b}}; \overline{\mathscr{b}'^2}; \tau\right) = -10log_{10}(\bar{\mathscr{b}}) + log_{10}\left(\overline{\mathscr{b}'^2}\right) + log_{10}(\tau) \tag{12}$$

is a function controlled by the statistical characteristics of the magnetopause location.

In any case, one needs to evaluate the average magnetopause location, $\overline{\mathscr{b}}$, the variance of the magnetopause location, $\overline{\mathscr{b}'^2}$, and the lifetime of the magnetopause fluctuations, τ, in order to quantify electromagnetic radial diffusion. Shue et al. (1998)'s magnetopause model provides a fast and accessible way to evaluate of these magnetopause parameters. In this model, the stand-off distance to the magnetopause is controlled by the dynamic pressure of the solar wind, and the orientation of the interplanetary magnetic field (IMF):

$$\mathscr{b} = \left(10.22 + 1.29\tanh\left(0.184 \times (B_z + 8.14)\right)\right)D_p^{-1/6.6} \quad (13)$$

where the solar wind dynamic pressure, D_p, is in nanopascals, and the north-south component of the IMF, B_z, is in nanoteslas (Shue et al., 1998). This model will be used in the following in order to quantify radial diffusion.

3. Quantification

3.1. Origin of Radial Diffusion Time Variability

In **equation (2)**, and thus in **equations (6)-(12)**, $A(t)$, and thus $\mathscr{b}(t)$, are considered to be realizations of a stationary stochastic process. In other words, it is assumed that the magnetopause location fluctuates randomly and that its statistical properties are time-independent. In practice, the signal $\mathscr{b}(t)$ does not correspond to realizations of a strictly stationary process, and the statistical properties of $\mathscr{b}$ are time varying. Thus, it is necessary to specify a sample window size to evaluate the statistical characteristics of the magnetopause location. As a result, **equation (11)** becomes:

$$log_{10}(D_{LL}/L^{10}) = F_T + 2log_{10}\Omega + C \quad (14)$$

where

$$F_T = -10log_{10}\left(\overline{\mathscr{b}}_T\right) + log_{10}\left(\overline{\mathscr{b}'^2}_T\right) + log_{10}(\tau_T) \quad (15)$$

and the subscript indicates that the quantity depends on the window size chosen, T. The moving average of the magnetopause location is:

$$\overline{\mathscr{b}}_T = \frac{1}{T}\int_{-T/2}^{T/2} \mathscr{b}(u)du \tag{16}$$

and the moving variance of the magnetopause location is:

$$\overline{\mathscr{b}'^2}_T = \frac{1}{T}\int^{T} \left(\mathscr{b}(u) - \overline{\mathscr{b}}_T(u)\right)^2 du \tag{17}$$

Thus, the time variability of the electromagnetic radial diffusion coefficient comes from the time variability of the statistical characteristics of the magnetopause location (average, variance, and lifetime). The radial diffusion coefficient increases 1) when the magnetopause average location decreases, 2) when the magnetopause fluctuations increase, or 3) when the lifetime increases (**equations (14)-(15)**). Which of these three possible effects has the most control over radial diffusion variability? In particular, why does the radial diffusion coefficient increase with Kp? To investigate this question, the three components of F_T were computed for the year 2013 with a one-hour window size ($T = 1h$). To pilot the magnetopause location (**equation (13)**) solar wind inputs with a one-min time resolution were extracted from NASA/GSFC's OMNI data set through OMNIWeb (https://omniweb.gsfc.nasa.gov/). The average and the variance were computed according to **equation (16)** and **(17)**, respectively, and the lifetime τ was determined by fitting the autocorrelation function to an exponential decay. The results are summarized by boxplots parameterized by the Kp index and they are presented **Figure 1**.

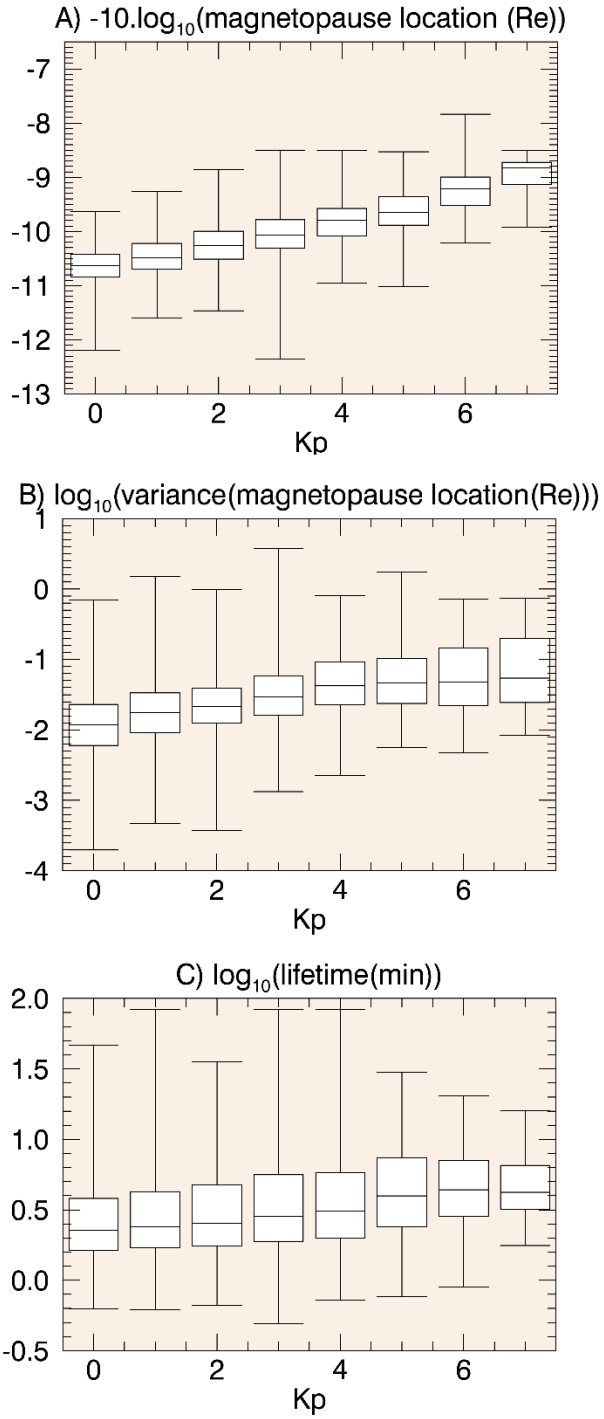

Figure 1: Magnitude of the three radial diffusion components that depend on the statistical characteristics of the magnetopause location, A) $-10log_{10}(\overline{\mathscr{b}})$, B) $log_{10}\left(\overline{\mathscr{b}'^2}\right)$, and C) $log_{10}(\tau)$ (see text for definitions). The ends of the whiskers correspond to the minimum and maximum values, the bottoms and the tops of the boxes are the lower and upper quartiles, and the bands inside the boxes are the medians. The sample window size chosen for the computations is one hour ($T = 1h$).

The **Figure 1** suggests that the magnitude of radial diffusion increases with the Kp index both because the average magnetopause location decreases with Kp (**Fig. 1A**) and because the fluctuations in magnetopause location increase with Kp (**Fig. 1B**). On the other hand, the fluctuation lifetime does not seem to depend much on Kp (**Fig. 1C**). It is typically of the order of a few minutes (< 10 min). Thus, for particles with drift periods that are such that $\Omega < 5\ mHz$, i.e., for radiation belt particles below a few MeV (e.g. Schulz and Lanzerotti, 1974, p.13), the assumption $\Omega\tau \ll 1$ is typically valid, and the **equation (11)** is a good approximation of the **equation (10)**.

3.2. Effect of the Sample Window Size on the Quantification of Radial Diffusion

The statistical characteristics of the magnetopause location presented **Figure 1** were determined using a sample window of one hour ($T = 1h$). To what extent does the choice of a sample window size affect the statistical characteristics of the magnetopause location, as summarized by F_T, thus, the magnitude of radial diffusion? To investigate this question, the function F_T was computed for 10 different sample window sizes over the year 2013: $T = [6\ min, 12\ min, 18\ min, 30\ min, 1\ h, 2\ h, 3\ h, 5\ h, 10\ h, 24\ h]$. The results are summarized by boxplots, and they are displayed **Figure 2**.

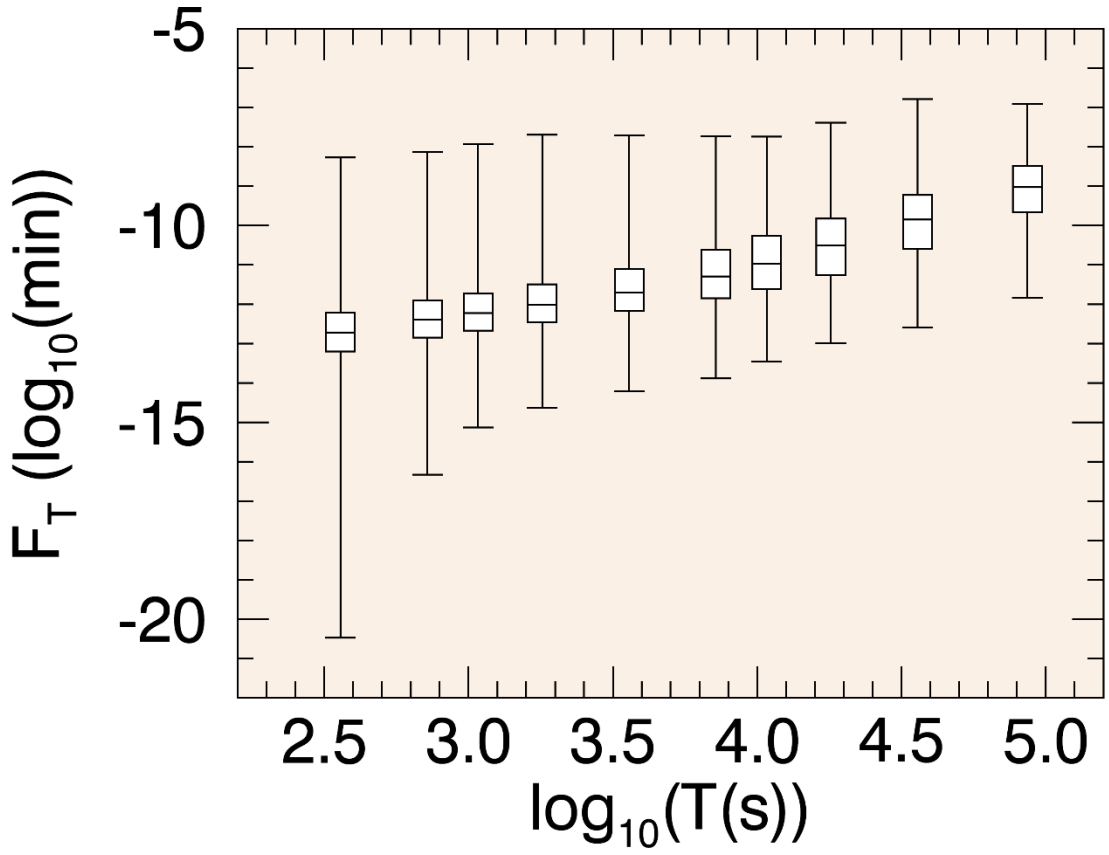

Figure 2: Magnitude of the parameter, F_T, which quantifies the effect of statistical characteristics of the magnetopause location on radial diffusion, as a function of the sample window size chosen for the statistical computations, T. The ends of the whiskers indicate the minimum and maximum values, the bottoms and the tops of the boxes are the lower and upper quartiles, and the bands inside the boxes are the medians.

The **Figure 2** shows that the magnitude of F_T decreases as the window size, T, decreases. This is because the average magnetopause location fits better the instantaneous value of the magnetopause location as the window size T decreases. Thus, the variance decreases as the window size decreases ($\overline{\mathscr{b}'^2} = 0$ for the asymptotic case in which T=0). A linear interpolation of F_T as a function of $log_{10}(T)$ yields that, on average:

$$\frac{dF_T}{d(log_{10}(T))} \cong 1.5 \tag{18}$$

with a standard deviation of 0.4.

When the objective is to quantify radial diffusion, the selected window size, T, must be consistent with the adiabatic invariant theory of magnetically trapped particles. Indeed, field fluctuations that evolve on timescales longer than the trapped population drift period conserve the third adiabatic invariant. On the other hand, asymmetric field fluctuations with characteristic times comprised between the bounce and the drift period violate the third invariant, driving radial diffusion (e.g., Northrop, 1963). Thus, the window size, T, must be such that all field fluctuations that are on timescales longer than the drift period are stored in $\overline{\mathscr{b}}$ while field fluctuations that are between the bounce and the drift period are in $\mathscr{b}'$. Given the one-minute time resolution of the input signal, the characteristic time for the variation of the field is always greater than the bounce period. Nonetheless, the window size, T, needs to be long in comparison with the trapped population drift period in order to compute the average, $\overline{\mathscr{b}}$:

$$T = \frac{2\pi k}{\Omega} \tag{19}$$

where k is a constant greater than one: $k > 1$. As a result, F_T is in fact dependent on the trapped population drift frequency. Indeed, combining **equations (18)** and **(19)** yields:

$$\frac{d\,F_T}{d(log_{10}(\Omega))} \cong -1.5 \tag{20}$$

As the kinetic energy increases, the drift frequency increases, thus, the magnitude of F_T decreases. In other words, the particle's drift motion is less and less sensitive to field fluctuations as the drift velocity increases (the discrepancies between $\overline{\mathscr{b}}$ and $\mathscr{b}(t)$ decrease as the drift period - thus T - decreases). Therefore, one should ideally tailor the computation of **equation (9)** according to the drift frequency. Yet, the expected dependence of radial diffusion on drift frequency is relatively weak. Indeed, for $\Omega\tau \ll 1$, combining **equation (20)** and **equation (14)** yields

$$d(log_{10}(D_{LL}/L^{10}))/d(log_{10}(\Omega)) \cong 0.5 \tag{21}$$

Thus, the magnitude of radial diffusion D_{LL} increases by about a factor 3 when the drift frequency increases by a factor 10. In comparison, for $\Omega\tau \gg 1$, assuming that the drift frequency dependence of F_T comes primarily from the variance, i.e., $dF/d(log_{10}(\Omega)) \approx d(log_{10}\left(\overline{\mathscr{b}'^2}\right))/d(log_{10}(\Omega))$:

$$d(log_{10}(D_{LL}/L^{10}))/d(log_{10}(\Omega)) \cong -1.5 < 0 \quad (22)$$

Thus, there is a cutoff in radial diffusion efficiency once the drift period becomes smaller than the fluctuation lifetime. Assuming that the order of magnitude obtained **equation (22)** is valid, the magnitude of radial diffusion D_{LL} decreases by about a factor 30 when the drift frequency increases by a factor 10.

While the selected window size needs to be consistent with adiabatic invariant theory, it also needs to be consistent with the mathematical assumptions underlying the model. In particular, field fluctuations must be regarded as realizations of a stationary process within the time interval considered. Such conditions are most likely achieved during magnetically quiet times, and/or when considering a relatively small time interval. Since the latter is not necessarily consistent with **equation (19)**, this poses a problem to radial diffusion quantification.

In the following, it is proposed to work with a sample window size of one hour: $T_{1h} = 1\ h$. A one-hour window is small enough to render radial diffusion variability with magnetic activity (as illustrated **Figure 1**) and to expedite the computations. It is also large enough to maintain sufficient data points to perform the required statistical analyzes. The average proportional relationship between the function, F_T, and the logarithmic of the drift frequency, $log_{10}(\Omega)$, is used to evaluate the appropriate value of F_T from F_{1h}. Combining **equations (14)**, **(19)** and **(20)** yields:

$$log_{10}(D_{LL}/L^{10}) = F_{1h} + 1.5\, log_{10}(2\pi k/T_{1h}) + 0.5\, log_{10}(\Omega) + C \quad (23)$$

for $\Omega < 5\ mHz$. Given the uncertainty in hands, the choice of the constant $k > 1$ is unimportant. It is set to $k = 10$ in the remainder. The radial diffusion coefficient is usually in $[day^{-1}]$ while the angular drift velocity is usually in $[mHz]$. As a result, a reformulation of the **equation (23)** is:

$$log_{10}(D_{LL}/L^{10}) = F_{1h} + 0.5\, log_{10}(\Omega) + 2.9 \quad (24)$$

where D_{LL} is evaluated in $[day^{-1}]$, F_{1h} is provided in $[log_{10}(min)]$, and Ω is in $[mHz]$.

4. Results and Comparison with Brautigam and Albert's Empirical Formula

The radial diffusion coefficients were computed for the year 2013 for a radiation belt population of angular drift velocity $\Omega = 1\ mHz$, following **equation (24)**. The time series is represented in

the **Figure 3** and it is compared to Brautigam and Albert's estimates for electromagnetic radial diffusion. The comparison highlights a) the overall good agreement between the two times series, b) the greater variability of the radial diffusion coefficients determined by the solar wind immediate time history, and c) some limitations of the statistical model. For instance, Brautigam and Albert's empirical formula has a lower threshold of $log_{10}(D_{LL}/L^{10}) = -9.325$ during quiet times ($Kp = 0$). The existence of a lower threshold for radial diffusion is not physical, since there would be no radial diffusion (i.e., $D_{LL} = 0$) if the electromagnetic fields were perfectly stationary. On the other hand, the radial diffusion coefficients determined by the solar wind immediate time history can be smaller, in accordance with theoretical expectations. The results were also binned according to the Kp index, and they are summarized in boxplots displayed **Figure 4**.

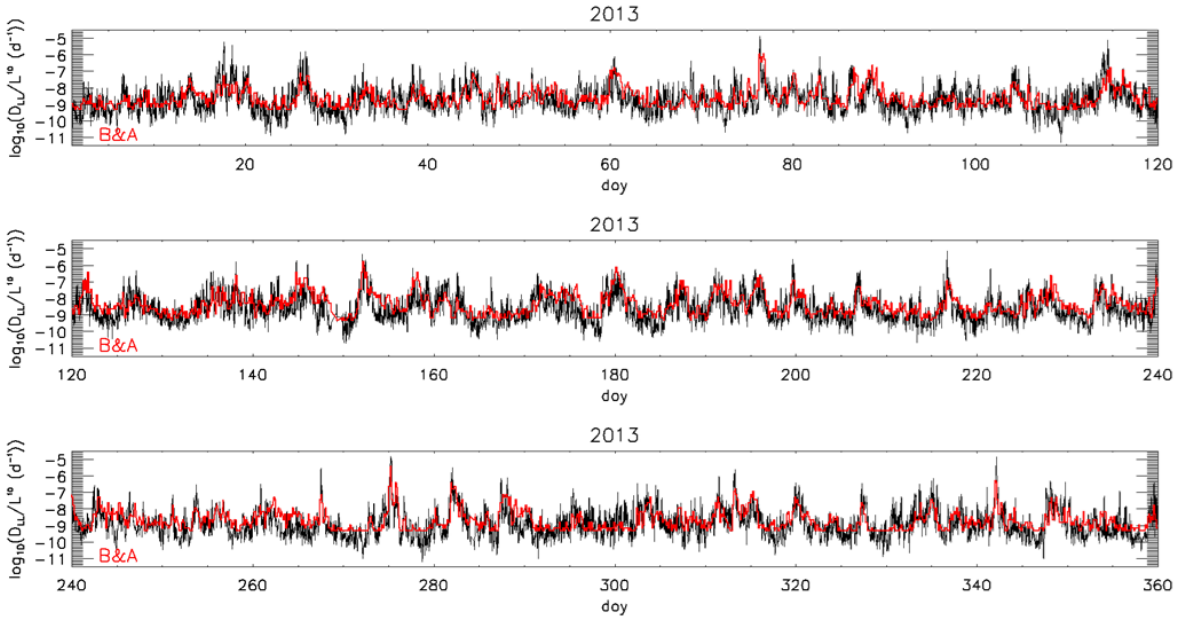

Figure 3. Electromagnetic radial diffusion as a function of the day of the year (doy) in 2013. The radial diffusion coefficients determined as a function of the solar wind immediate time history are in black. The radial diffusion coefficients determined by Brautigam and Albert (2000)'s empirical formula (B&A) are in red.

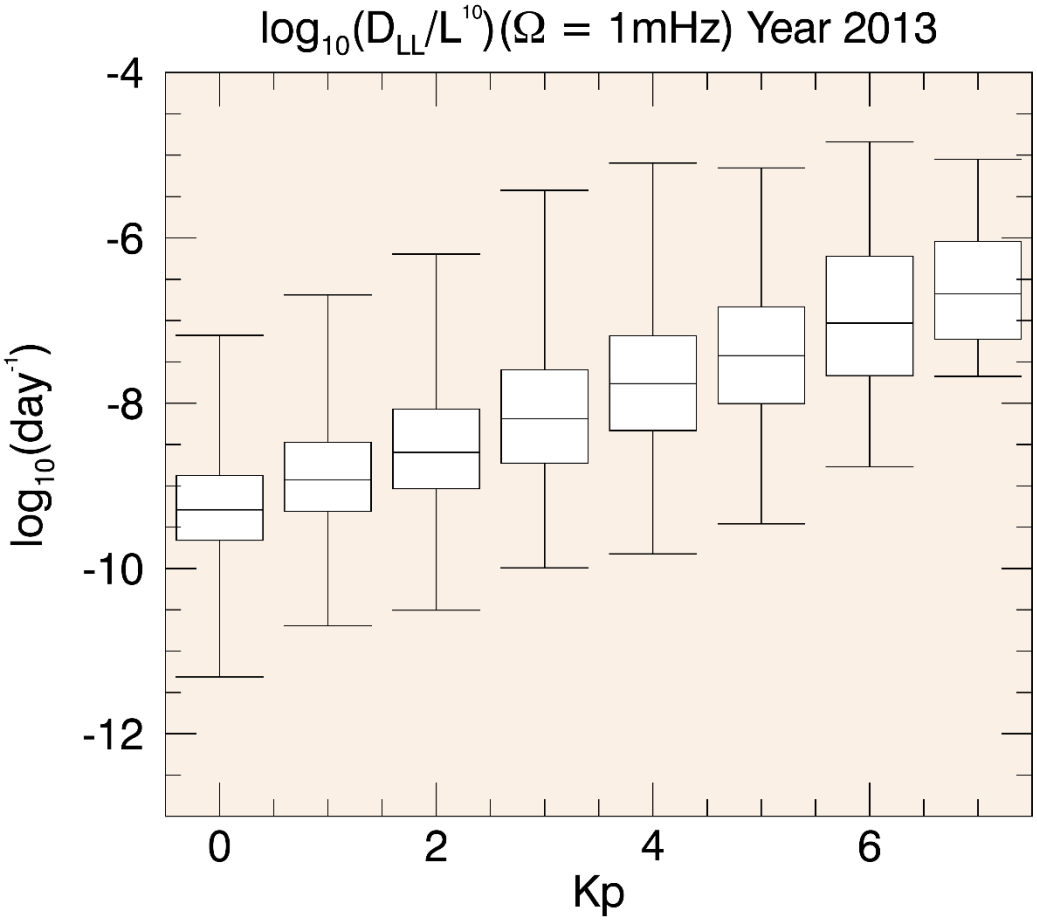

Figure 4. Statistical characterization of the electromagnetic radial diffusion magnitude for the year 2013, as a function of the Kp index, for a population of angular drift velocity $\Omega = 1\ mHz$. The ends of the whiskers indicate the minimum and maximum values, the bottoms and the tops of the boxes are the lower and upper quartiles, and the bands inside the boxes are the medians. The values were computed for the year 2013 according to **equation (24)**, with a one-minute time resolution.

A linear interpolation of the medians per Kp index for the electromagnetic radial diffusion magnitude yields:

$$log_{10}(D_{LL}/L^{10}) = -9.309 + 0.377 \times Kp \ \ [log_{10}(day^{-1})] \qquad (25)$$

This interpolation is remarkably similar to the one obtained by Brautigam and Albert (2000) (**equation (1)**). The difference in the intercepts is < 1% while the slope as a function of Kp is only 25% smaller than the one found by Brautigam and Albert. One reason for such similarity may be that both estimates rely on the same theoretical toy model for the electromagnetic fields. Yet, the

radial diffusion coefficients obtained by Lanzerotti and Morgan (1973) and Lanzerotti et al. (1978) were based on an analysis of magnetic field fluctuations measured by at ground level (at L=4) and at synchronous equatorial altitude (L=6.6). In these analyzes, the power spectrum of the fluctuations was fitted to a functional form ($P \propto \Omega^{-s}$, with s between 1 and 3). On the other hand, the numerical evaluations proposed here rely on solar wind measurements, and the autocorrelation function is fitted to an exponential decay (**equation (7)**). Because τ is found to be very small, both fitting methods are usually equivalent: In both cases, the power spectrum decreases as $\propto \Omega^{-2}$ over a large frequency range.

The time series of the three parameters constitutive of F_{1h} together with the magnitude of $log_{10}(D_{LL}/L^{10})$ computed for the year 2013 for a radiation belt population of angular drift frequency $\Omega = 1\ mHz$ is accessible online (http://doi.org/10.5281/zenodo.3625265).

5. Discussion

The pros and cons of the method developed in this paper are summarized in the following.

First, the method faces the same theoretical limitations as the ones underlying Brautigam and Albert's formula for electromagnetic diffusion. Namely: It relies on an oversimplified electromagnetic field model (a "toy model"). Even when fitting the simplified Mead (1964)'s magnetic field formula to a basic external magnetic field model, such as the one developed by Tsyganenko (1989), discrepancies appear. There is also little doubt that the response of the magnetospheric fields to fluctuations in the magnetopause location is more complicated than what is actually described by the theoretical picture provided here. The proposed radial diffusion coefficients are also limited at both high and low L values. Indeed, at high L values, the electromagnetic field is expected to be more distorted and more variable than predicted. In that context, the distinction between L and L^* is also necessary (e.g. Roederer & Lejosne, 2018). At low L values, electrostatic radial diffusion is probably very important (e.g., O'Brien et al., 2016; Selesnick et al., 2016), and yet such diffusion process is not taken into account here.

Even so, the resulting coefficients binned as a function of the Kp index display remarkable agreement an empirical law that is generally considered standard. Furthermore, the theoretical picture presented here provides physical insights on the origin of radial diffusion variability: radial diffusion increases as the Kp index increases both because the magnetic field is more compressed (thus, the average asymmetry increases), and because it fluctuates more (thus, the variance of the asymmetry increases). The model also describes how electromagnetic radial diffusion varies with drift frequency. When the drift frequency increases, the part of the radial diffusion coefficient that explicitly depends on energy (third term **equation (9))** increases, until it plateaus (for $\Omega\tau \gg 1$). The term that quantifies the effect of the statistical characteristics of the magnetopause, F_T, is also indirectly controlled by drift frequency. Indeed, the signal decomposition into an average and a fluctuating part requires the definition of a reference. The reference, set by adiabatic invariant theory, is the drift period. Field variations that evolve on time scales greater than the drift period are part of the average (that is, they do not violate the third invariant), while field variations that

evolve on time scales shorter than the drift period constitute the fluctuating part of the signal. As the drift frequency increases, the average describes more and more precisely the signal instantaneous values, and the variance decreases. Thus, F_T decreases as the drift frequency increases. As a result, there is a sweet spot in drift frequency at which radial diffusion is maximal, Ω_{max}. A derivation of **equation (9)** with respect to $log_{10}(\Omega)$ yields $\Omega_{max} \approx 0.6/\tau$. With a fluctuation lifetime, τ, of the order of a couple of minutes, $\Omega_{max} \approx 5\ mHz$. Even so, for $\Omega\tau \ll 1$, as is typically the case for most radiation belt particles, the resulting dependence of electromagnetic radial diffusion on drift frequency is relatively weak ($D_{LL} \propto \sim\Omega^{0.5}$). Such feature greatly simplifies radial diffusion quantification.

In the most general case, radial diffusion is controlled by the asymmetry in the electromagnetic field fluctuations (e.g., Northrop, 1963; Lejosne et al., 2012). Thus, quantifying radial diffusion requires monitoring electromagnetic field fluctuations. While previous work attempted to monitor the asymmetry of the magnetic field at geostationary orbit (Lejosne et al., 2013), this new model presents the advantage of being operational. Leveraging a toy model for the fields, the asymmetry of the field is controlled by the magnetopause, whose location is a function of solar wind parameters. Interestingly enough, it is not the first time that the solar wind is chosen to drive radial diffusion (Li et al., 2001). From a technical standpoint, the advantage of working with such a simple model is that it highlights some of the challenges that need to be addressed to quantify radial diffusion accurately, regardless of the model complexity. In particular, this work highlights some of the difficulties related to the analysis of non-stationary field fluctuations.

Acknowledgments

The work of S.L. was performed under JHU/APL Contract No. 922613 (RBSP-EFW) and NASA Grant Award 80NSSC18K1223. The use of NASA/GSFC's Space Physics Data Facility's OMNIWeb (https://omniweb.gsfc.nasa.gov/) service and OMNI data is acknowledged.

References

Ali, A. F., Malaspina, D. M., Elkington, S. R., Jaynes, A. N., Chan, A. A., Wygant, J., and Kletzing, C. A. (2016), Electric and magnetic radial diffusion coefficients using the Van Allen probes data, J. Geophys. Res. Space Physics, 121, 9586– 9607, doi:10.1002/2016JA023002.

Beutier, T., and Boscher, D. (1995), A three-dimensional analysis of the electron radiation belt by the Salammbô code, J. Geophys. Res., 100(A8), 14853– 14861, doi:10.1029/94JA03066.

Brautigam, D.H., Albert, J.M. (2000), Radial diffusion analysis of outer radiation belt electrons during the October 9, 1990, magnetic storm. J. Geophys. Res., 105(A1), 291–309. https://doi.org/10.1029/1999JA900344

Drozdov, A. Y., Shprits, Y. Y., Aseev, N. A., Kellerman, A. C., and Reeves, G. D. (2017), Dependence of radiation belt simulations to assumed radial diffusion rates tested for two empirical models of radial transport, Space Weather, 15, 150– 162, doi:10.1002/2016SW001426.

Fälthammar, C.-G. (1965), Effects of time-dependent electric fields on geomagnetically trapped radiation. J. Geophys. Res., 70(11), 2503–2516. https://doi.org/10.1029/JZ070i011p02503

Fälthammar, C.-G. (1968), Radial diffusion by violation of the third adiabatic invariant, in Earth's Particles and Fields, edited by B. M. McCormac, pp. 157–169, Reinhold, New York.

Fei, Y., Chan, A.A., Elkington, S.R., & Wiltberger, M. J. (2006). Radial diffusion and MHD particle simulations of relativistic electron transport by ULF waves in the September 1998 storm, J. Geophys. Res., 111, A12209, doi:10.1029/2005JA011211.

Glauert, S. A., Horne, R. B., & Meredith, N. P. (2018). A 30-year simulation of the outer electron radiation belt. Space Weather, 16, 1498– 1522. https://doi.org/10.1029/2018SW001981

Horne, R. B., Glauert, S. A., Meredith, N. P., Boscher, D., Maget, V., Heynderickx, D., and Pitchford, D. (2013), Space weather impacts on satellites and forecasting the Earth's electron radiation belts with SPACECAST, Space Weather, 11, 169– 186, doi:10.1002/swe.20023.

Kim, K.-C., Shprits, Y., Subbotin, D., and Ni, B. (2011), Understanding the dynamic evolution of the relativistic electron slot region including radial and pitch angle diffusion, J. Geophys. Res., 116, A10214, doi:10.1029/2011JA016684.

Lanzerotti, L. J., & Morgan, C. G. (1973). ULF geomagnetic power near L = 4: 2. Temporal variation of the radial diffusion coefficient for relativistic electrons, J. Geophys. Res., 78(22), 4600–4610, doi:10.1029/JA078i022p04600.

Lanzerotti, L. J., Webb, D. C., & Arthur, C. W. (1978). Geomagnetic field fluctuations at synchronous orbit 2. Radial diffusion, J. Geophys. Res., 83(A8), 3866–3870, doi:10.1029/JA083iA08p03866.

Lejosne, S., Boscher, D., Maget, V., and Rolland, G. (2012), Bounce-averaged approach to radial diffusion modeling: From a new derivation of the instantaneous rate of change of the third adiabatic invariant to the characterization of the radial diffusion process, J. Geophys. Res., 117, A08231, doi:10.1029/2012JA018011.

Lejosne, S., Boscher, D., Maget, V., and Rolland, G. (2013), Deriving electromagnetic radial diffusion coefficients of radiation belt equatorial particles for different levels of magnetic activity based on magnetic field measurements at geostationary orbit, J. Geophys. Res. Space Physics, 118, 3147– 3156, doi:10.1002/jgra.50361.

Lejosne, S. (2019). Analytic expressions for radial diffusion. Journal of Geophysical Research: Space Physics, 124, 4278– 4294. https://doi.org/10.1029/2019JA026786

Lejosne, S., and Kollmann, P. (2019), Radiation Belt Radial Diffusion at Earth and Beyond. Earth and Space Science Open Archive. https://doi.org/10.1002/essoar.10501074.1

Li, X., Temerin, M., Baker, D.N., Reeves, G.D., and Larson, D., (2001), Quantitative prediction of radiation belt electrons at geostationary orbit based on solar wind measurements, Geophys. Res. Lett., 28 (9), 1887-1890. https://doi.org/10.1029/2000GL012681

Li, Z., Hudson, M., Patel, M., Wiltberger, M., Boyd, A., and Turner, D. (2017), ULF wave analysis and radial diffusion calculation using a global MHD model for the 17 March 2013 and 2015 storms, J. Geophys. Res. Space Physics, 122, 7353– 7363, doi:10.1002/2016JA023846.

Mann, I.R., et al. (2016), Explaining the dynamics of the ultra-relativistic third Van Allen radiation belt. Nature Phys. 12:978–983. https://doi.org/10.1038/nphys3799 3154 3155

Mann, I.R., et al. (2018). Reply to 'The dynamics of Van Allen belts revisited'. Nature Physics, 14(2), 103–104. https://doi.org/10.1038/nphys4351

Mead, G. D. (1964). Deformation of the geomagnetic field by the solar wind, J. Geophys. Res., 69(7), 1181– 1195, doi:10.1029/JZ069i007p01181.

Northrop, T.G. (1963), *The Adiabatic Motion of Charged Particles*. Wiley Interscience, Hoboken, N. J. ISBN-13: 978-0470651391.

O'Brien, T. P., Claudepierre, S. G., Guild, T. B., Fennell, J. F., Turner, D. L., Blake, J. B., Clemmons, J. H., and Roeder, J. L. (2016), Inner zone and slot electron radial diffusion revisited, Geophys. Res. Lett., 43, 7301– 7310, doi:10.1002/2016GL069749.

Ozeke, L. G., Mann, I. R., Murphy, K. R., Jonathan Rae, I., and Milling, D. K. (2014), Analytic expressions for ULF wave radiation belt radial diffusion coefficients, J. Geophys. Res. Space Physics, 119, 1587– 1605, doi:10.1002/2013JA019204.

Roederer, J. G., & Lejosne, S. (2018). Coordinates for representing radiation belt particle flux. J. Geophys. Res. Space Physics, 123, 1381– 1387. https://doi.org/10.1002/2017JA025053

Schulz, M., and Eviatar, A. (1969), Diffusion of equatorial particles in the outer radiation zone, J. Geophys. Res., 74(9), 2182– 2192, doi:10.1029/JA074i009p02182.

Schulz, M. and Lanzerotti, L.J. (1974), Particle Diffusion in the Radiation Belts. Springer-Verlag Berlin Heidelberg. https://doi.org/10.1007/978-3-642-65675-0

Selesnick, R. S., Su, Y.-J., and Blake, J. B. (2016), Control of the innermost electron radiation belt by large-scale electric fields, J. Geophys. Res. Space Physics, 121, 8417– 8427, doi:10.1002/2016JA022973.

Shprits Y.Y., et al. (2018), The dynamics of Van Allen belts revisited. Nature Physics, 14, 102–103. https://doi.org/10.1038/nphys4350

Shue, J.-H., et al. (1998), Magnetopause location under extreme solar wind conditions, J. Geophys. Res., 103(A8), 17691– 17700, doi:10.1029/98JA01103.

Tsyganenko, N. A. (1989), A magnetospheric magnetic field model with a warped tail current sheet, Planet. Space Sci., 37(1), 5–20.

Tu, W., Li, X., Chen, Y., Reeves, G. D., and Temerin, M. (2009), Storm-dependent radiation belt electron dynamics, J. Geophys. Res., 114, A02217, doi:10.1029/2008JA013480